Iterative techniques for eigenvalue solutions of damped structures coupled with fluids

AIAA 2002-1391

Adrien Bobillot and Étienne Balmès *

École Centrale Paris - MSSMat, 92295 Châtenay-Malabry, France

When computing the dynamic response of a structure, eigenvalue computations play a central role. For structures with internal compressible fluids, a pressure formulation leads to non symmetric real matrices so that one typically uses complex eigenvalue solvers. Moreover, if one considers structures containing damped materials, the matrices become complex.

The present paper discusses a class of partial eigenvalue solvers that are applicable to these problems. The main characteristics of the proposed techniques are the use of iterations on real subspaces, basis enrichment using residues computed at a particular step, and the separate factorization of the real part of the structure and fluid stiffness matrices. These ingredients are key to the significant speedup obtained over a standard complex eigenvalue solver. The paper discusses energy norms which are used to evaluate convergence by estimating the size of residues, and how these residues are used to enrich the basis for the next iteration. The effectiveness of using standard modal approximations of the exact solutions to start the iterations is finally discussed.

Evaluations in terms of speed and accuracy are shown for a 57,000 DOFs model of a PSA Peugeot Citroën oil pan, with a constrained viscoelastic layer, and for a model of the main cryogenic stage of Ariane 5 consisting of 88,000 DOFs. Computations are performed using the Structural Dynamics Toolbox for MATLAB taking the MSC/NASTRAN complex eigenvalue solver as reference for comparisons.

Introduction

Eigenvalue solutions are critical for the analysis of the resonant properties of structures and for modal approximations of transient dynamics.

Real eigenvalue solvers for elasticity problems have received considerable attention and the associated theory is well described in textbooks[1,2] .

Problems with viscous and hysteretic damping and problems with fluid structure coupling lead to quadratic eigenvalue problems

$$\left(M\lambda^2 + D\lambda + K + iB\right)\{\phi\} = \{0\} \qquad (1)$$

which are typically solved by canonical transformation to first order form[3,4] .

It is rightfully shown in Ref.[4] that paying attention to the block structure of the first order form of the quadratic eigenvalue problem can lead to significant speedup. This paper pushes the idea further and introduces Ritz basis solvers with residue iteration that are applicable to eigenvalue problems with multiple fields.

The case of a viscoelastically damped structure coupled with a compressible fluid is considered here to show the general applicability of the proposed eigenvalue solvers. The problem is described using displacement, velocity and viscoelastic relaxation fields for the structure and pressure and pressure rate for the fluid. While one still has a first order eigenvalue problem, the proposed eigensolvers make use of the specific block structure and are thus significantly more efficient than standard solvers.

The first section summarizes the models used to describe viscoelastic damping and elasto-acoustic coupling. The second part of the paper analyses classical and new eigenvalue solvers. The last section analyzes performance and convergence for the cases of an oil pan made of a viscoelastic sandwich shell and a model of the Ariane 5 main cryogenic stage.

Damping and Fluid Models

To illustrate the proposed eigenvalue solution strategy, one will consider models of damped structures, fluid-structure interaction and damped structures coupled with fluid. The associated models are described in this section.

Viscoelastic damping

The basic assumption of linear viscoelasticity[5] is the existence of a relaxation function $h(t)$ such that the stress is obtained as a convolution with the strain history

$$\sigma(t) = \int_0^{+\infty} \varepsilon(t-\tau)h(\tau, T, \sigma_0)d\tau. \qquad (2)$$

Using the Laplace transform, one obtains an equivalent representation where the material is now charac-

*Professor, Department of Mechanical Engineering

terized by the *Complex Modulus E* (transform of the relaxation function)

$$\sigma(s) = E(s, T, \sigma_0)\varepsilon(s) = (E' + iE'')\varepsilon(s). \quad (3)$$

For all practical purposes, one can thus, in the frequency domain, deal with viscoleasticity as a special case of elasticity where the material properties are complex and depend on frequency, temperature, prestress and possibly other environmental factors.

In practice, the complex modulus is determined experimentally using dynamic excitation. For a given set of material test results, analysis requires knowledge of $E(s)$ for arbitrary values of s or at least of the frequency on the Fourier axis ($s = i\omega$). Three approaches are typically used :

- $E(i\omega)$ is interpolated from tabulated material test data.
- $E(s)$ is represented by a rational fraction

$$E(s) = E_0 \frac{1 + \alpha_1 s + ... + \alpha^{nn} s^{nn}}{1 + \beta_1 s + ... + \beta^{nd} s^{nd}}. \quad (4)$$

  Some particular reduced forms of a rational fraction may be used in practice.
- $E(s)$ is represented using another analytical representation, in particular fractional derivatives[6] .

When proper care is taken, all three approaches are capable of closely approximating material test data. They thus have the same "physical" validity. The differences are really seen in how each representation can be integrated in FEM solvers and in the validity of extrapolations outside the tested material behavior range. On the later point, the actual process used to obtain the parameters has a strong influence, it may thus be easier to obtain a good model with a particular representation even if that representation is not inherently better.

Dependence on environmental factors (temperature, pre-stress, ...) should `a priori` be arbitrary. In practice however, one generally assumes that environmental factors only act as shifts on a reduced frequency[7] . Tests thus seek to characterize a master curve $E_m(s)$ and a shift function $\alpha(T, \sigma_0)$ describing the modulus as

$$E(s, T, \sigma_0) = E_m(\alpha(T, \sigma_0)s). \quad (5)$$

Since the strain energy is a linear function of the constitutive law parameters $E_i(s, T, \sigma_0)$, one can build a representation of the dynamic stiffness as a linear combination of constant matrices

$$[Z(E_i, s)] = \left[Ms^2 + K_e + \textstyle\sum_i E_i(s, T, \sigma_0) \frac{K_{vi}(E_0)}{E_0} \right]. \quad (6)$$

This representation is the basis used to develop practical direct frequency response solvers for viscoelastic vibration problems[8] .

Of particular interest for eigenvalue solutions are the cases where E_i have a rational fraction expression. An arbitrary rational fraction (4) that is proper and has distinct poles, can be represented as a sum of first order rational fractions

$$E(s) = E_\infty - \left(\sum_{j=1}^{n} \frac{E_j}{s + \omega_j} \right). \quad (7)$$

Using a method similar to the canonical transformation described by Komzsik[4] for converting quadratic problems to linear problems, (6) is transformed into a higher order linear problem by introducing an internal viscoelastic relaxation field $q_{vj} = -\frac{E_j}{(s+\omega_j)} q$. For a single q_{vj}, (6) thus takes the form

$$\left[\begin{bmatrix} M & 0 & 0 \\ 0 & M & 0 \\ 0 & 0 & M \end{bmatrix} s + \begin{bmatrix} 0 & -M & 0 \\ K_e + E_\infty K_v & 0 & K_v \\ E_j M & 0 & \omega_j M \end{bmatrix} \right] \begin{Bmatrix} q \\ sq \\ q_v \end{Bmatrix} = \begin{Bmatrix} 0 \\ F \\ 0 \end{Bmatrix}. \quad (8)$$

A particular case is produced when the complex modulus is considered to be a constant, i.e. $E(s) = E_0(1 + \eta j)$, which corresponds to hysteretic damping. If loss factors are introduced in both the elastic (η_e) and the damping core (η_v), the first order problem to be solved is simply

$$Ms^2 q + ((1 + \eta_e j)K_e + (1 + \eta_v j)K_v)q = F. \quad (9)$$

Fluid structure coupling

The type of coupling which is considered in this paper is based on elasto-acoustic, which applies to structures containing a compressible non-weighting fluid with or without free surface, as described in figure 1. The finite element formulation for this type of problem can be written as in Ref.[9]

$$\left[\begin{bmatrix} K & -C \\ 0 & F \end{bmatrix} + s^2 \begin{bmatrix} M & 0 \\ C^T & K_p \end{bmatrix} \right] \begin{Bmatrix} q \\ p \end{Bmatrix} = [Z_{str-fl}] \begin{Bmatrix} q \\ p \end{Bmatrix} = \begin{Bmatrix} F \\ 0 \end{Bmatrix}, \quad (10)$$

with q the displacements of the structure, p the pressure variations in the fluid and F the external load applied to the structure, where

$$\begin{array}{c} \int_{\Omega_S} \sigma_{ij}(u)\epsilon_{ij}(\delta u)dx \Rightarrow \delta q^T K q \\ \int_{\Omega_S} \rho_S u.\delta u dx \Rightarrow \delta q^T M q \\ \frac{1}{\rho_F} \int_{\Omega_F} \nabla p \nabla \delta p dx \Rightarrow \delta p^T F p \\ \frac{1}{\rho_F c^2} \int_{\Omega_F} p \delta p dx \Rightarrow \delta p^T K_p p \\ \int_{\Sigma} p \delta u.n dx \Rightarrow \delta q^T C p \end{array} \quad (11)$$

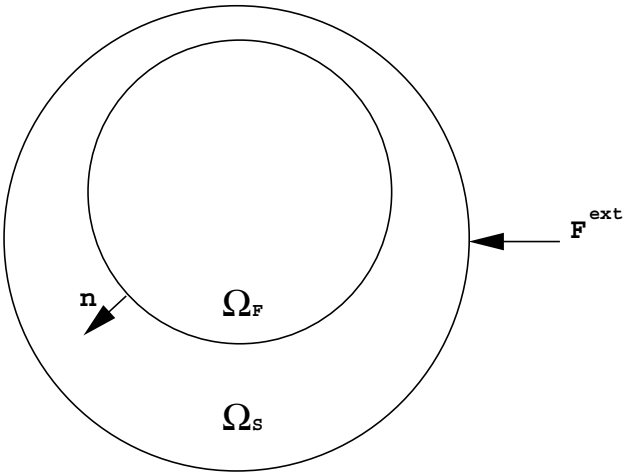

Fig. 1 Fluid-structure interaction scheme

In the implementation used for applications, the coupling term C is computed using fluid/structure coupling elements with one integration point at the center of gravity of each element. When structural and fluid meshes do not match at boundaries, pairing of elements needs to be done. For each fluid element F_i, one takes the center of gravity $G_{f,i}$ (figure 2), and searches the solid element S_i which is facing the center of gravity, in the direction of the normal to the fluid element F_i. The projection of $G_{f,i}$ on the solid element, P_i, belongs to S_i, and one computes the reference coordinate r and s of P_i in S_i (if S_i is a quad4, $-1 < r < 1$ and $-1 < s < 1$). Thus one knows the weights that have to be associated to each node of S_i. The coupling term will thus associate the DOFs of F_i to the DOFs of S_i, with the corresponding weights.

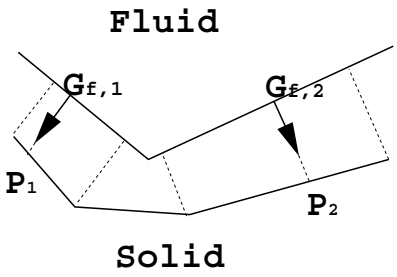

Fig. 2 Non-matching meshes

Damped structures coupled with fluids

One now considers a structure with viscoelastic damping coupled with a fluid. The equation to be solved can be obtained by substituting the stiffness matrix in (10) by the expression developed in (8), corresponding to a viscoelastic behavior. The resulting equation thus couples the five fields : displacement q, velocity sq, viscoelastic relaxation q_v, pressure fluctuation p and pressure fluctuation rate sp as follows

$$\left[\begin{bmatrix} M & 0 & 0 & 0 & 0 \\ 0 & M & 0 & 0 & 0 \\ 0 & 0 & M & 0 & 0 \\ 0 & 0 & 0 & K_p & 0 \\ 0 & C^T & 0 & 0 & K_p \end{bmatrix} s + \begin{bmatrix} 0 & -M & 0 & 0 & 0 \\ K_e + E_\infty K_v & 0 & K_v - C & 0 & \\ \alpha M & 0 & \omega_j M & 0 & 0 \\ 0 & 0 & 0 & 0 & -K_p \\ 0 & 0 & 0 & F & 0 \end{bmatrix}\right] \begin{Bmatrix} q \\ sq \\ q_v \\ p \\ sp \end{Bmatrix} = \begin{Bmatrix} 0 \\ F_e \\ 0 \\ 0 \\ 0 \end{Bmatrix} \tag{12}$$

The eigenvalue problem of interest is thus non-symmetric and high order with 2 times the number of structural DOFs, 2 times the number of fluid DOFs and one or more times that number of viscoelastic relaxation DOFs (accurate representation of many viscoelastic materials requires 5 to 10 terms in (7) and thus as many relaxation fields).

Thus although (12) is associated with a first order eigenvalue problem, standard solvers will perform poorly because it is associated with a larger number of DOFs. This limitation motivates the work presented here.

Eigenvalue problems

Overview of classical methods

All the problems detailed in the previous sections can be written as generalized eigenvalue problems with constant matrices of the form

$$[A]\{\theta_j\} = [B]\{\theta_j\}\lambda_j, \tag{13}$$

Solvers for these problems are either complete solvers which compute all the eigensolutions and are applicable only for small matrices, or partial solvers which seek the eigensolutions in a particular frequency zone (typically low frequency poles near the imaginary axis).

Our focus is on large order problems, so that complete solvers are not applicable. We will thus detail in this section different types of partial solvers. The inverse iteration method shows the fundamental recurrence that allows partial mode estimation. Standard generalizations are the subspace and Lanczos methods[1–4] , and we introduce the new concept of Ritz methods with residue iterations. The main computational costs of these methods are associated with identical tools: factorization, forward-backward substitution, projection, complete resolution on the reduced problem. Their differences are thus mainly related to their respective convergence rate.

Inverse iteration method

The fundamental principle of this method is to solve the inverse problem of (13)

$$[A]^{-1}[B]\{x_j\} = \frac{1}{\lambda_j}\{x_j\}, \tag{14}$$

by building a recurrence of the form

$$\left\{x^{(n)}\right\} = [A]^{-1}[B]\left\{x^{(n-1)}\right\}. \tag{15}$$

The ratio of the non-zero components of $\frac{\left\{x^{(n)}\right\}}{\left\{x^{(n-1)}\right\}}$ converge to the inverse of the smallest eigenvalue of (13) $\frac{1}{\lambda_1}$, c.f.[1] and $\left\{x^{(n)}\right\}$ converge to the corresponding eigenvector θ_1. The following eigenvalues are then obtained by a process of orthogonal deflation with respect to the eigenvectors already computed. This method is far less efficient than the methods described below, and must be used only to determine very few eigenvalues in case of numerical problems associated to the other methods.

Generalizations of the inverse iteration seek several eigenvectors at once. They are based on the assumption that an accurate approximation of the solution of (13) can be found in the subspace spanned by the columns of a rectangular reduction basis T (with N rows and $NR << N$ columns). The approximate eigenvalues of (13) in the subspace spanned by T are given by $\{\phi_j\}_{approx} = T\{\phi_j\}_R$ with $\{\phi_j\}_R$ the solution of the reduced eigenvalue problem (solved by a complete solver)

$$[T]^T[A - \lambda_{j,R}B][T]\{\theta_j\}_R = \{0\}. \tag{16}$$

The accuracy of the approximate solution thus only depends on the subspace spanned by T.

Subspace method

The subspace method builds a sequence of bases $T^{(0)}$, $...T^{(n)}$ which span the subspaces E^0, $...E^n$. The recurrence form at step k is a simple generalization of the inverse iteration method

$$T^{(k+1)} = [A]^{-1}[B]T^{(k)}, \tag{17}$$

These subspaces are intended to converge to the subspace E^∞ containing the p first eigenvectors of (13). The vectors of each subspace E^k must be orthogonalized to avoid E^k to collapse to a vector corresponding to the first eigenvector. One can note that, unlike in the Lanczos method, the size of E^k does not increase during the iterations. Typically, one sets subspace size to $\min(p + 12, 2p)$.

The iterations are stopped by computing the modes in the E^k and checking the size of an appropriate dynamic residual. The dynamic residual is however not used directly.

Lanczos method

The principle of the Lanczos method[1,3,4] is to build a subspace by successive inverse iterations on a unique vector z_0. From this vector, one builds the Krylov sequence

$$T = \left[z_0,\ (A^{-1}B)z_0, (A^{-1}B)^2 z_0,\ ...\right], \tag{18}$$

using a recursive orthogonalization scheme to keep the different vectors orthogonal (this scheme corresponds to a conjugate gradient search). This subspace converges rapidly to a subspace containing the first eigenvectors of (13), which are computed using a complete solver on the reduced system.

Problems arise when z_0 does not excite certain modes, which happens in particular for cases with multiple modes. Only numerical oscillations, or the use of several vectors as starting points, will make these modes appear in the subspace. For real eigenvectors, the Sturm sequences technique[1] allows to check if one did not miss an eigenvalue, but for complex modes, such a technique does not exist.

In the next section, the starting point is a basis containing at least the reference real modes, which makes the risk of missing an eigenvalue minimal.

Ritz method with residue iterations

To introduce the new Ritz method with residue iteration, one first considers the one field eigenvalue problem

$$\left[K - \omega_j^2 M\right]\{\phi_j\} = \{0\}. \tag{19}$$

Starting from a basis $T^{(0)}$, whose selection will be discussed later, the following steps are performed at iteration k

1. Projection of (19) on $T^{(k)}$ and complete resolution (for example by a QR method) of the reduced eigenvalue problem ${T^{(k)}}^T\left[K - \omega_{j,R}^2 M\right]T^{(k)}\{\phi_{j,R}\} = 0$,

2. Computation of the load residuals associated to the basis $T^{(k)}$

$$\left\{R_{j,L}^{(k)}\right\} = \left[K - \omega_{j,R}^2 M\right]T^{(k)}\{\phi_{j,R}\} \neq 0 \tag{20}$$

   using the fact that $T^{(k)}\phi_{j,R}$ does not exactly satisfy (13).

3. Computation of the displacement residuals

$$\left\{R_{j,D}^{(k)}\right\} = \left[\hat{K}\right]^{-1}\left\{R_{j,L}^{(k)}\right\} \tag{21}$$

   where $\left[\hat{K}\right]$ is a mass shifted stiffness matrix ($\hat{K} = K + \alpha M$) when rigid body modes pose problems. The static flexible response would be another alternative (see[1] on iterations in presence of rigid body modes). In practice, when load residuals are complex (complex solution), they are separated into a real and a complex part. The displacement residuals are then obtained by $R_{j,D}^{(k)} = \left[\hat{K}\right]^{-1}\left[\Re\left\{R_{j,L}^{(k)}\right\}\ \Im\left\{R_{j,L}^{(k)}\right\}\right]$.

4. Evaluation of the relative strain energy error indicator (of course a kinetic energy criterion could

alternatively be defined, or a mix of both)

$$\epsilon_j^{(k)} = \frac{\|\left\{R_{j,D}^{(k)}\right\}\|^2{}_K}{\|T^{(k)}\{\phi_{j,R}\}\|_K^2} = \frac{\|\left\{R_{j,D}^{(k)}\right\}\|^2{}_K}{\omega_{j,R}^2}$$

(the modeshapes are normalized with respect to the mass and stiffness matrices).
For complex cases, a singular value decomposition is performed on $\left[\Re\left\{R_{j,L}^{(k)}\right\}\ \Im\left\{R_{j,L}^{(k)}\right\}\right]^T K\left[\Re\left\{R_{j,L}^{(k)}\right\}\ \Im\left\{R_{j,L}^{(k)}\right\}\right]$ (which is a 2 by 2 matrix), thus extracting the direction generating the highest residual energy. This direction is defined by two scalars a and b which give the vector $\left\{R_{j,D}^{(k)}\right\} = a\Re\left\{R_{j,L}^{(k)}\right\} + b\Im\left\{R_{j,L}^{(k)}\right\}$ associated to the highest error. For complex problems this vector is used in step [5], thus leading to iterations on real subspaces.

5. Basis completion:
$\epsilon^{(k)}{}_j > Tol \Rightarrow T^{(k+1)} = \left[T^{(k)}, \left\{R_{j,D}^{(k)}\right\}\right]$.

These steps are repeated until every ϵ_j is less than a user-fixed tolerance. In practice, the residues that complete the basis $T^{(k)}$ need to be orthogonalized with respect to $T^{(k)}$ to avoid numerical conditioning problems linked to strong vector collinearity.

Since the method is iterative, the number of steps needed is dependent on the initial basis $T^{(0)}$. For real eigenvalue computations, the best candidate is the result of a short Lanczos run which gives good eigenvectors estimates but not always the desired accuracy. For complex computations of structures with hysteretic damping (9), a minimal starting basis includes the normal modes corresponding to $\eta = 0$.

This method can be viewed as a compromise between the Lanczos and the subspace method. Indeed, the size of the subspace spanned by $T^{(k)}$ increases at each iteration step as in the Lanczos method, but the recurrence proceeds similarly to the subspace method. Indeed, one can note that the displacement residuals that are used to complete $T^{(k)}$ lay in the subspace spanned by $\left[\left[\hat{K}\right]^{-1}\left[K - \omega_{j,R}^2 M\right]T^{(k)}\right]$, which is similar to (17).

Ritz method with residue iterations - Application to multiple field problems

The objective of this section is to generalize the residue iteration strategy to problems with multiple fields (8), (10) or (12).

Considering viscoelastic structure coupled with a fluid (12), one seeks to approximate the five fields q, sq, q_v, p and sp. The first three fields are related to the displacement in the structure q, and the last two fields are related to the pressure fluctuation p. One thus considers two subspaces for the iterations: one related to displacement (spanned by T_q) and the other related to pressure (spanned by T_p).

Starting from basis

$$T^{(0)} = \begin{bmatrix} T_q^{(0)} & 0 & 0 & 0 & 0 \\ 0 & T_q^{(0)} & 0 & 0 & 0 \\ 0 & 0 & T_q^{(0)} & 0 & 0 \\ 0 & 0 & 0 & T_p^{(0)} & 0 \\ 0 & 0 & 0 & 0 & T_p^{(0)} \end{bmatrix}, \quad (22)$$

the following steps are performed at iteration k

1. Projection of (12) on $T^{(k)}$ and complete resolution (for example by a QR method) of the reduced eigenvalue problem. the approximate fields $T_q^{(k)}q_R$, $T_q^{(k)}sq_R$, $T_q^{(k)}q_{v,R}$, $T_p^{(k)}p_R$ and $T_p^{(k)}sp_R$ are thus obtained.

2. Computation of the load residuals for pressure

$$\begin{aligned}\left\{R^{(k)}{}_{p,j,L}\right\} = C^T s^2 T_q^{(k)} q_{j,R} + \\ K_p s^2 T_p^{(k)} p_{j,R} + F T_p^{(k)} p_{j,R}\end{aligned} \quad (23)$$

and displacement

$$\begin{aligned}\left\{R^{(k)}{}_{q,j,L}\right\} = Ms^2 T_q^{(k)} q_{j,R} + \\ [K_e + E_\infty K_v] T_q^{(k)} q_{j,R} + \\ K_v T_q^{(k)} q_{v,j,R} - C T_p^{(k)} p_{j,R}\end{aligned} \quad (24)$$

which characterize the fact that the approximate solution does not verify exactly the block equations (rows 2 and 5) of the eigenvalue problem associated with (12). The other block rows are not considered because they are exactly verified.

3. Computation of the displacement residuals for q $\left\{R_{q,j,D}^{(k)}\right\} = [K_0]^{-1}\left\{R_{q,j,L}^{(k)}\right\}$, where $[K_0] = [K_e + K_v + \alpha M]$ is the mass shifted stiffness matrix of the structure (in case of rigid body modes), and for p $\left\{R_{p,j,D}^{(k)}\right\} = \left[\hat{K}_p\right]^{-1}\left\{R_{p,j,L}^{(k)}\right\}$, where $\left[\hat{K}_p\right]$ is a mass shifted stiffness matrix for the fluid (in case of rigid body modes).

3. Evaluation of the relative strain energy error indicators
$\epsilon_{q,j}^k = \frac{\|\left\{R^k{}_{q,j,D}\right\}\|^2{}_{K_0}}{\|T_q^k\{q_{j,R}\}\|_{K_0}^2}$,
$\epsilon_{p,j}^k = \frac{\|\left\{R^k{}_{p,j,D}\right\}\|^2{}_{K_p}}{\|T_p^k\{p_{j,R}\}\|_{K_p}^2}$

4. Bases completion:
$\epsilon^{(k)}{}_{q,j} > Tol \Rightarrow T_q^{(k+1)} = \left[T_q^{(k)}, \left\{R^{(k)}{}_{q,j,D}\right\}\right]$,
$\epsilon^{(k)}{}_{p,j} > Tol \Rightarrow T_p^{(k+1)} = \left[T_p^{(k)}, \left\{R^{(k)}{}_{p,j,D}\right\}\right]$.

As in the previous section, these steps are repeated until every ϵ_j is less than a user-fixed tolerance and

the residues are orthogonalized with respect to $T^{(k)}$ to avoid numerical conditioning problems linked to strong vector collinearity. For complex vectors, one uses a singular value decomposition to retain a real subspace as done in the single field problem.

For the starting basis, one uses a typical approximation for coupled problems combining real eigenvectors of the uncoupled structure and fluid problems.

The first advantage of the proposed approach is that one only needs to factor K_0 (which has the size of the structure problem) and $\hat{K}_p$ (which has the size of the fluid problem). The ability to use approximation (uncoupled solutions) also leads to fast convergence when coupling is weak.

Applications

Sample models and test configurations

The proposed methods were tested on two models.

The first model, a PSA Peugeot Citroën oil pan shown in figure 6, has in the nominal case 5561 elements with 8507 nodes (33003 DOFs). When a sandwich layer is added (used for viscoelastic and hysteretic studies), the model has 14227 elements and 12931 nodes (57457 DOFs). The nominal mesh is generated with I-DEAS and the additional elements needed to model the sandwich design are generated using the MATLAB based *Structural Dynamics Toolbox*[10] . The fluid model contains 7666 elements for 1470 DOFs (related to pressure fluctuation).

The second model, provided by EADS Launcher Vehicles, represents a part of the main cryogenic stage of the Ariane 5 launcher, including two tanks as shown in figure 8. It has 5832 structural elements (33708 DOFs) and 56112 fluid elements (54341 DOFs).

Comparisons made in the following sections were performed running NASTRAN[7] version 70.7 and an implementation of the proposed methods using SDT 4.1[10] . NASTRAN element matrices were imported into the SDT to allow direct comparison of results. The only difference is in the fluid/structure coupling formulation which is not exported by NASTRAN.

CPU times are given for runs on an SGI R10000 processor. Although the computations were performed on a 128 processor Origin 2000, a single processor was used. The only parrallel aspect was thus the shared memory and I/O.

Damped structures

Computational times

Table 1 shows a breakdown of CPU times for various analyses of the sandwich design of the oil pan.

Basic steps are first compared : factorization of the real stiffness, forward/backward substitution, and nomal (real) mode computations. Both codes use similar multifrontal sparse factorization routines and the differences in factorization time can in part be attributed to different settings in the approach used to create the elimination trees. The SDT spends more time optimizing the factorization which results in faster forward/backward substitution. The resulting computational times for normal mode solution are very similar.

Table 1 CPU times in seconds of some key steps. Resolution of (8) and (9) (Oil pan, 57159 DOFs, N.A. : not applicable)

	NASTRAN	SDT
Model assembly	41	N.A.
Factorization of K	50	90
Forward/back. substitution	5.2	2.7
20 normal modes	273	252
20 cpx. modes Hysteretic (Total)	1420-1447	286-332 $Tol = 10^{-5}$
20 cpx. modes viscoelastic (Total)	N.A.	333-1737 $Tol = 10^{-5}$

For solving the complex eigenvalue problem with a constant loss factor (hysteretic damping), NASTRAN uses a complex Lanczos algorithm, while the *Ritz method with residue iterations* is used by the SDT (with $Tol = 10^{-5}$ and $T^0 = [\phi_{1..20}]$ in the present case). For NASTRAN, computational times for complex modes include the factorization of a complex matrix and resolution time. For SDT, they include factorization of a real matrix, normal modes computation and the iterative complex mode refinement.

For loss factors ranging from $\eta_{steel} = 1\%$ to 5% and $\eta_{visco} = 5$ to 30% for the steel and the damping core respectively, the speedup is significant (from 4.3 to 5). One can note that the proposed solver is sensitive to the damping level which is an expected result since for low damping the real modes used as $T^{(0)}$ are fairly accurate approximations of the complex ones (the time needed to create $T^{(0)}$ is included in the complex mode solution time).

The extension to a viscoelastically damped model affects the cost, but the resolution time remains reasonable and well below the Lanczos solver of NASTRAN. The range of times shown in this case corresponds to different temperatures (detailed in the physical study) with convergence being slower in cases with higher damping.

Physical study

The computations concerning viscoelastic damping are performed using a 3 parameter model for the Young modulus of the viscoelastic core

$$E(s,T) = E_{max}\frac{\alpha_T s + \omega_{min}}{\alpha_T s + \frac{E_{max}\omega_{min}}{E_{min}}}, \qquad (25)$$

where

$$log_{10}(\alpha_T) = -c_1 \frac{T - T_{ref}}{T - (Tref - c2)}, \qquad (26)$$

and $E_{max} = 10GPa$, $E_{min} = 8GPa$, $\omega_{min} = 300Hz$, $c_1 = 2$, $T_{ref} = 70^oC$, $c_2 = 100^oC$. Figure 3 illustrates for a temperature of 30^oC, the evolution of $E(s)$ with the frequency, in magnitude and phase. As expected, this plot shows a optimal value of the loss factor at the maximum slope of the storage modulus.

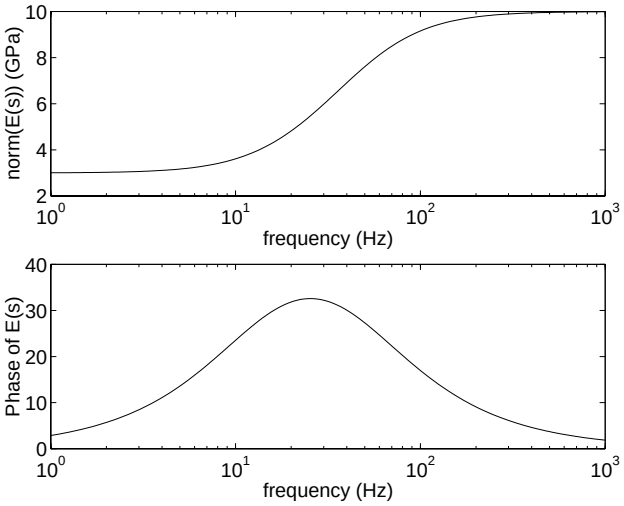

Fig. 3 Evolution of $E(s,T)$ with the frequency at $T = 30^oC$. Top: Amplitude, Bottom: Phase angle.

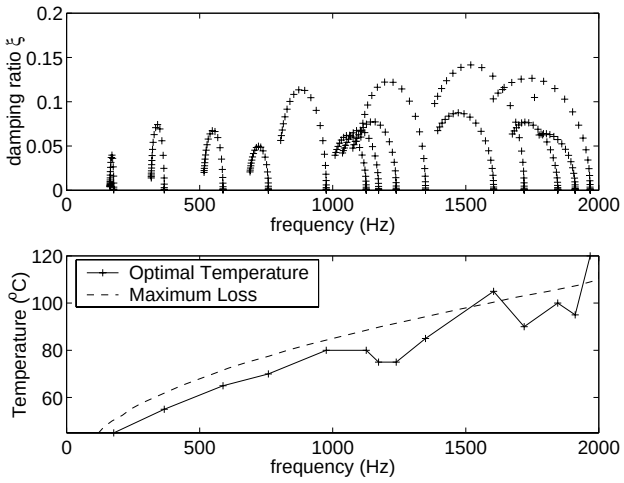

Fig. 4 Top: Evolution of ξ with the temperature for flexible modes 7 to 20,Bottom: Maximum loss temperature for flexible modes 7 to 20.

The top part of figure 4 shows the evolution of pole locations for temperatures ranging from $T = 10$ to 120^oC. This tracking of poles allows to study the evolution of the temperature inducing maximum loss in the structure for each mode. The bottom part of figure 4 shows that this optimum differs from the temperature at which the material dissipates most (corresponding to the maximum of $\frac{\Re E(s,T)}{\Im E(s,T)}$). This shows the importance of structural effects in damping design.

Figure 5 presents an example of convergence of the iterative method for hysteretic damping introduced in the steel ($\eta_{steel} = 1\%$) and the visco layer ($\eta_{visco} = 1000\%$). An excessive loss factor has been introduced in the viscoelastic core in order to illustrate convergence needs. One can see that a basis containing the normal (real) modes $\phi_{1..20}$ overestimates the modal dampings ξ_j. Adding the static response to the viscoelastic loads ($\hat{K}^{-1}K_v\phi_{7..20}$ for flexible modes) improves the results but still overestimates modal dampings. The *Ritz method with residue iterations* starting from $T_0 = \left[\phi_{1..20},\ \hat{K}^{-1}K_v\phi_{7..20}\right]$ gives an estimate of both the modal damping ratios and the frequencies at .01% relative error after only 3 iterations.

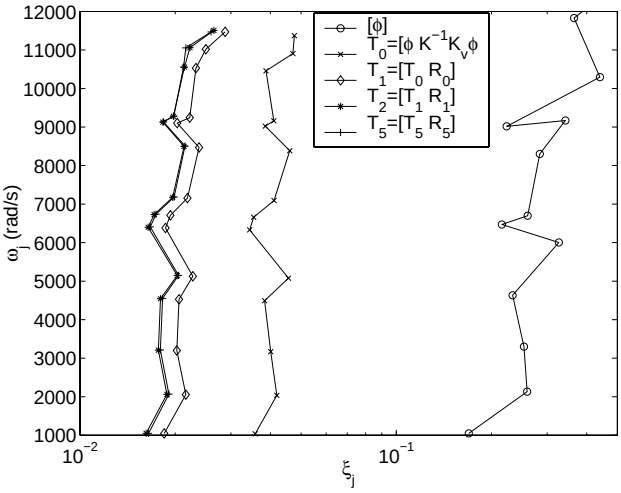

Fig. 5 Convergence of the complex poles for $\eta_{steel} = 0.01$ and $\eta_{visco} = 10$ (excessive value to illustrate convergence needs)

Fluid-Structure Coupling

Evaluations of the proposed method were performed on the oil pan and Ariane 5 model.

Figures 6 illustrates the pressure fluctuations at fluid nodes and the standard nodal displacement of structure nodes. Correlation between results from

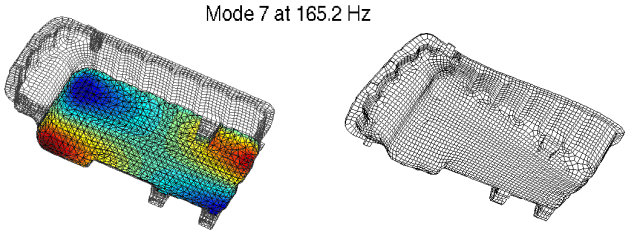

Fig. 6 First flexible mode of the oil pan model with fluid. Left: Pressure fluctuations in the fluid, Right: Displacement of the structure.

NASTRAN and the SDT is shown in figure 7, which represents the mass weighted MAC on both the displacements q and the pressure p and the relative errors on frequencies for flexible modes 7 to 20. It indicates

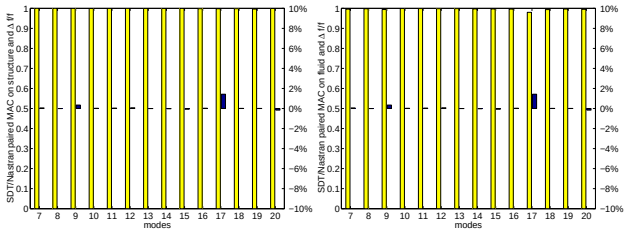

Fig. 7 MAC_m and relative error on frequency between SDT ans NASTRAN.

an excellent correlation of the modes, with all MACs greater than .98 and almost zero frequency errors, except for mode 17 for which SDT gives a frequency 1.5% greater than NASTRAN. This marginal difference is attributed to the different strategy used in building the fluid/structure coupling matrices.

Table 2 summarizes the respective CPU times for NASTRAN and the SDT. The complex Lanczos algorithm used by NASTRAN requires the factorization of the global matrix (c.f. (10)), whereas the *Ritz method with residue iterations* factorizes the real structure and fluid stiffnesses separately, which is far less costly. For this application, the speedup obtained by the Ritz method is greater than 2 even though the SDT solver for normal modes is somewhat less efficient than that of NASTRAN.

Table 2 CPU times in seconds of some key steps. Resolution of (10) (Oil pan, 31745 structure DOFs, 1470 fluid DOFs, N.A. : not applicable)

	NASTRAN	SDT
Factorization of K	129	fluid: 2 structure: 11
20 fluid modes	N.A.	8
20 structure modes	N.A.	90
20 coupled modes (Total)	300	143 $Tol = 10^{-5}$

The second application was performed on the Ariane 5 main cryogenic stage model. Figure 8 represents the structure displacements and pressure in the fluid, while table 3 summarizes CPU times for some key steps. Computations were not performed with NASTRAN because the job exceeded available system capacity.

Fluid and damped structure case

The final application is the resolution of (12) for the sandwich design of the oil pan with oil. The modulus used for the sandwich core is

$$E(s) = 10\text{GPa}\Big(1 - \frac{a}{s+w}\Big) \qquad (27)$$

with $w = 1.133\ 10^4$rad/s and $a = w/5$.

Table 4 summarizes only the SDT computational times because NASTRAN does not solve this type of

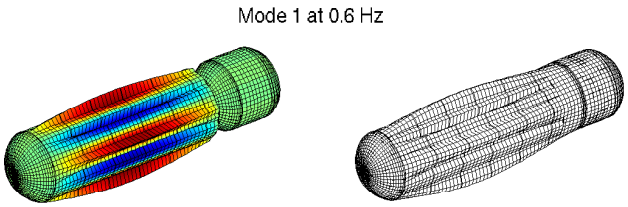

Fig. 8 First mode of the Ariane 5 main cryogenic stage model (without damping) with fluid. Left: Pressure fluctuations in the fluid, Right: Displacement of the structure.

Table 3 SDT CPU times in seconds of some key steps. Resolution of (10) (Ariane 5, 33708 structure DOFs, 54341 fluid DOFs)

Factorization of K	fluid: 88.6 structure: 17.7
20 fluid modes	217.6
20 structure modes	100.7
20 coupled modes (Total)	597 $Tol = 10^{-5}$

problems. In the present case the system to solve concerns non-symmetric matrices of size 174417 and the resolution is performed within less than 19 min.

Table 4 SDT CPU times in seconds. Resolution of (12) (Oil Pan, 57159 structure DOFs, 1470 fluid DOFs, $Tol = 10^{-4}$,)

Factorization of K	fluid: 2 structure: 90
20 fluid modes	8
20 structure modes	342
20 coupled modes (Total)	1128 $Tol = 10^{-4}$

Figure 9 shows the evolution of the reduction bases size, as well as the relative strain energy errors for both the displacement and the pressure fields (c.f. section "Ritz method with residue iterations - Application to multiple field problems"). Starting from the bases $T_q^{(0)} = [\phi_{str,1..20}]$ and $T_p^{(0)} = [\phi_{fl,1..20}]$ containing the uncoupled structure and fluid modes, one can see that both errors drop below the tolerance defined (10^{-4}) while the bases size increase gradually. At starting point, the error on the pressure field is above 100%, which shows how the uncoupled modes basis gives poor estimates of the solution.

Conclusion

This paper introduced a *Ritz method with residue iterations* which allows the computation of damped structures (viscoelastic and hysteretic damping) coupled with fluid. The notions of model reduction (Ritz

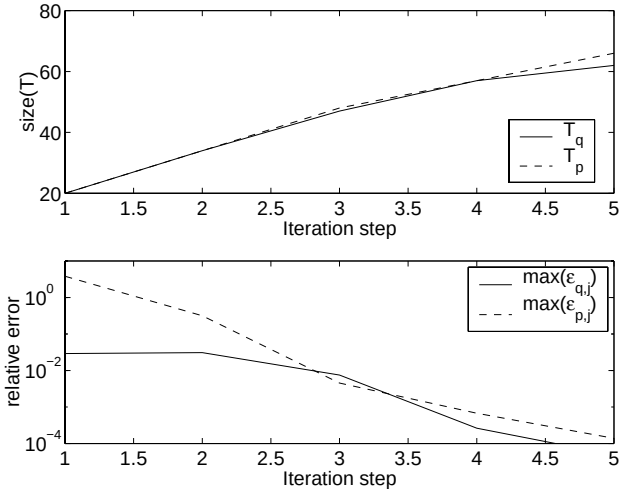

Fig. 9 Convergence for the displacement q and the pressure p for the *Ritz method with residue iterations* with $Tol = 10^{-4}$ and viscoelastic damping.

analysis) and residue iterations, on which the method is based, are quite general and allow the creation of iterative solvers for many problems arising in modal analysis (computing Minimum Dynamic Residual Expansion[11] , modal sensitivities[12] , FRFs[13] and FRF sensitivities, ...).

The paper illustrates different applications of the method, and shows its efficiency. Indeed, for complex eigenvalue solvers, the proposed method only needs to use factorizations of real stiffness matrices. Concerning the fluid/structure coupling case, the separate factorization of the structure and fluid matrices also provides significant speedup. Finally, for the viscoelastic damping case, the eigenvalue computation cost does not significantly increase from the hysteretic damping case.

References

[1]Géradin, M. and Rixen, D., *Mechanical Vibrations. Theory and Application to Structural Dynamics.*, John Wiley & Wiley and Sons, 1994, also in French, Masson, Paris, 1993.

[2]Bathe, K., *Finite Element Procedures in Engineering Analysis*, Prentice-Hall Inc., Englewood Cliffs, NJ, 1982.

[3]Tran, D., "Méthode de Lanczos par bloc appliquée aux problèmes de vibration des structures amorties," *Revue européenne des éléments finis*, Vol. 4, No. 1, 1995, pp. 33–54.

[4]Komzsik, L., "Implicit computational solution of generalized quadratic eigenvalue problems," *Finite Elements in Analysis and Design*, Vol. 37, 2001, pp. 799–810.

[5]Salençon, J., *Viscoélasticité*, Presse des Ponts et Chaussés, Paris, 1983.

[6]Bagley, L. and Torvik, P., "Fractional calculus - A different approach to the analysis of viscoelastically damped structures," *AIAA Journal*, Vol. 21, No. 5, 1983, pp. 741–748.

[7]MSC/NASTRAN, *Quick Reference Guide 70.5*, MacNeal Shwendler Corp., Los Angeles, CA, February, 1998.

[8]Balmès, E. and Bobillot, A., "Analysis and design tools for structures damped by viscoelastic materials," *IMAC*, February 2002.

[9]Morand, H. J.-P. and Ohayon, R., *Fluid-Structure Interaction: Applied Numerical Methods*, J. Wiley & Sons 1995, also in french, Masson, Paris, 1992.

[10]Balmès, E., *Structural Dynamics Toolbox 4.1 (for use with MATLAB)*, http://www.sdtools.com, February 2001.

[11]Bobillot, A. and Balmès, E., "Solving Minimum Dynamic Residual Expansion and Using Results for Error Localization," *IMAC*, 2001, pp. 179–185.

[12]Bobillot, A. and Balmès, E., "Iterative Computation of Modal Sensitivities," *Submitted to AIAA Journal*, 2001.

[13]Kergourlay, G., Balmès, E., and Clouteau, D., "Interface model reduction for efficient FEM/BEM coupling," *ISMA, Leuven*, September 2000.